DOI: 10.7860/IJARS/2024/70329.3007

Review Article

Surgery Section

Classical Radiological Signs and Appearances of Surgical Importance with Corresponding Operative Pictures: A Pictorial Review

RAVIKUMAR KALYANBHAI BALAR[1], NATASHA NANDA[2], ABHIJIT SHARADCHANDRA JOSHI[3]

ABSTRACT

The advent of various new-age radiological modalities over the years has brought about paradigm shifts in diagnostics for clinicians all over the world. These advancements have refined medical practice immeasurably. Accurate diagnosis have, in turn, enabled surgeons to administer appropriate and timely surgical therapy to their patients. The timeline of path-breaking radiological inventions from X-rays to Ultrasonics, Computed Tomography (CT), Magnetic Resonance Imaging (MRI), and beyond, bears living testimony to the role that preoperative imaging plays in a surgeon's daily life. The present review paper nostalgically remembers and acknowledges the pioneers of this remarkable journey. Additionally, it shares the authors' experiences with classical radiological signs and appearances correlated with their corresponding surgical 'first look' pictures from some of the rare and interesting cases the authors have encountered over the years. The present cases exhibit diverse presentations, clinical signs, radiological findings and diagnosis. The crucial role played by radiology in clinicians' daily lives, particularly in accurately diagnosing rare conditions, underscores the need to report these diverse cases.

Keywords: Accurate, Computed tomography, Diagnosis, Magnetic resonance, Ultrasonics, X-rays

INTRODUCTION

In the present review, the authors have highlighted several diagnostic imaging signs of surgical significance based on their experience, which have enriched our practice of the fine art of surgery. Some of these signs may not be widely recognised, but they exhibit classical diagnostic appearances. Additionally, the authors have included an operative 'first look' or subsequent surgical step, along with a specimen picture of the same patient, alongside the corresponding imaging images to emphasise the important association between the two. The authors, hereby, present 13 surgical conditions [Table/Fig-1-13] from their experience, in which the science of radiology aided them in achieving a specific, accurate and comprehensive preoperative diagnosis, thereby facilitating timely and precise surgical therapy for these patients.

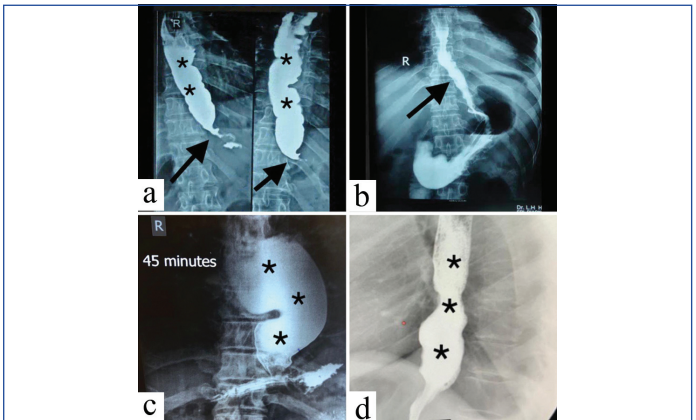

[Table/Fig-1]: Achalasia Cardia (AC): a-d) Shows how classically a simple imaging modality like Barium Swallow (BS) diagnoses the present rare condition; a) Classical bird's beak sign (black arrows) and proximal dilated oesophagus (black asterisks); b) Postoperative (post cardiomyotomy) image of the same patient which reveals the free flow of oral contrast across the surgical myotomy (black arrow), unlike image a; c) BS image of another patient with a classical appearance of advanced AC- a condition called sigmoid achalasia, wherein the very dilated oesophagus loses its normal axis and appears 'S' shaped (black asterisks), like the sigmoid colon!; d) Postmyotomy image of the same patient which shows correction of the oesophageal axis and normalisation of its caliber (black asterisks).

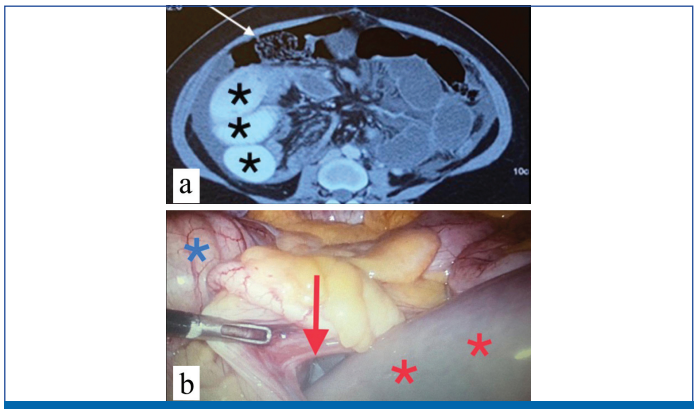

[Table/Fig-2]: Right paraduodenal hernia: a) Axial cut of Contrast-enhanced Computed Tomography (CECT) abdomen showing dilated small bowel loops (black asterisks) posterior to the ascending colon (white arrow); b) Operative 1st look image of the same patient showing small bowel loops (red asterisks) entering the fossa of Waldeyer (red arrow) behind the ascending colon (blue asterisk).

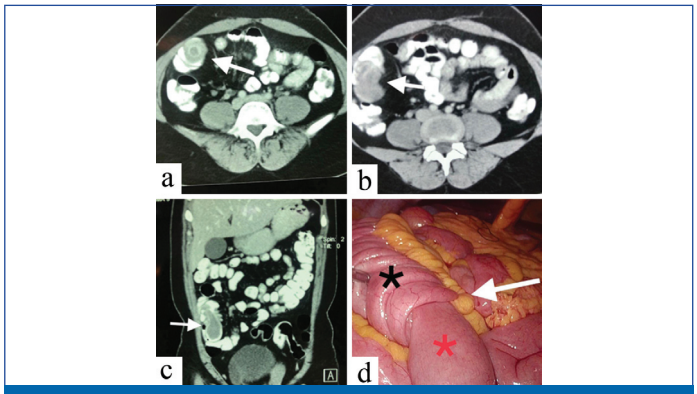

[Table/Fig-3]: Ileo-ileal intussusception: a) (Axial view of CECT) reveals the classical bull's eye sign also called target sign (white arrow); b) Axial view; and c) Coronal view showing classical sausage sign (white arrow) in the same patient; d) The 1st look operative image of the same patient shows the intussusceptum (red asterisk) entering the intussusception (black asterisk) at the point of intussusceptions (white arrow).

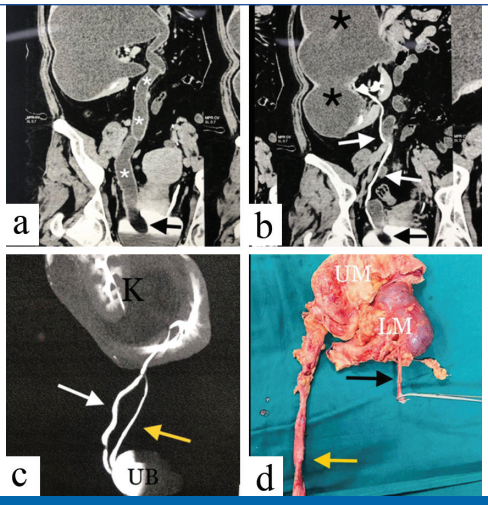

[Table/Fig-4]: Right duplex moiety: This refers to duplex kidney formation as a result of early divisions of the ureter during embryogenesis. It is characterised by the presence of two pelvicalyceal systems with partial or complete duplication of the ureters. a) CT urography (coronal view) shows the dilated ureter of the non functioning upper moiety (white asterisks) with a ureterocele at its lower end (black arrow); b) CT urography (coronal view) shows the non functioning upper moiety (black asterisks) along with the normal caliber ureter of the lower moiety (white arrows) and the ureterocele (black arrow) at the lower end of the other dilated ureter; c) Three dimensional (3D) reconstruction of CT urography showing two right kidney moieties with one dilated (white arrow) and one normal caliber (yellow arrow) ureter; d) Operative specimen with both the moieties along with the dilated (yellow arrow) and normal (black arrow) ureters.

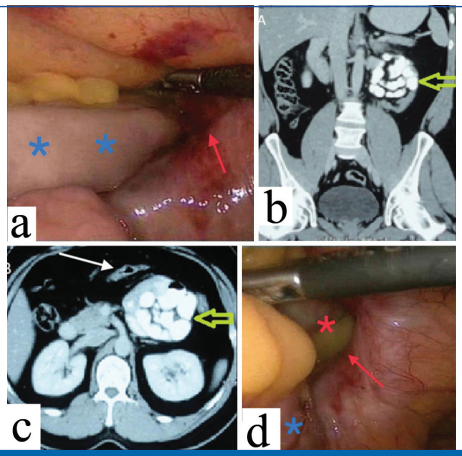

[Table/Fig-5]: Left paraduodenal hernia: a) First look operative image of the same patient revealing small bowel (blue asterisks) trapped in the left paraduodenal defect (red arrow); b,c) Coronal and axial views of CECT abdomen revealing clumped contrast filled loops of small bowel (green arrow) behind the descending colon (white arrow); d) Small bowel (blue asterisks) being reduced from the fossa of Landzert (red asterisk) through the left paraduodenal defect (red arrow).

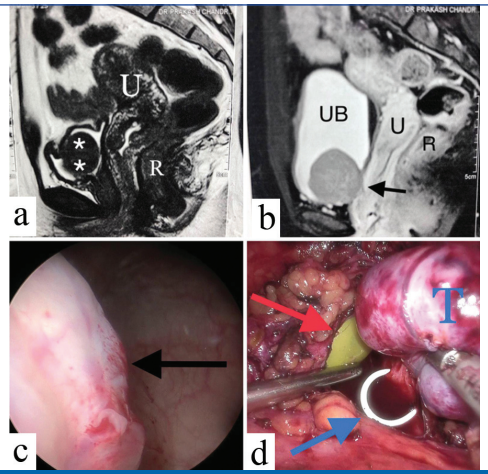

[Table/Fig-6]: Urinary bladder outlet tumour: a) MRI pelvis (sagittal view) showing the bladder outlet tumour (white asterisks) anterior to the uterus and rectum; b) Sagittal view of CECT pelvis of the same patient revealing the tumour (black arrow) within the urinary bladder; c) Cystoscopic view of the bladder tumour (black arrow); d) Intraoperative image of laparoscopic resection of the tumour which shows Foley's catheter (red arrow) and D-J stent (blue arrow) in situ. These are seen after opening up of the urinary bladder, during laparoscopic resection of the tumour.

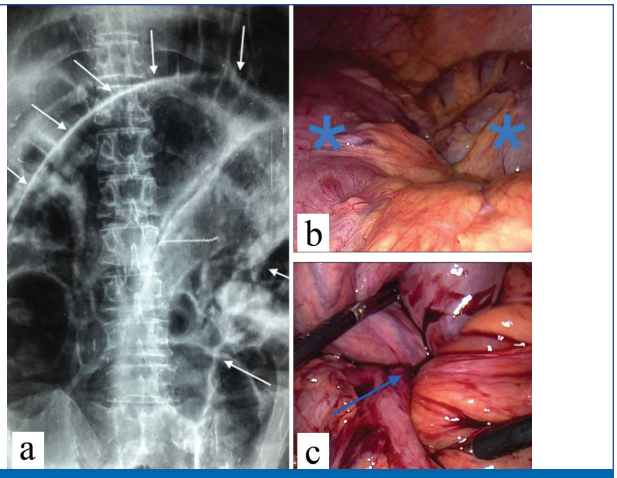

[Table/Fig-7]: Sigmoid volvulus: a) Plane X-ray abdomen {Anteroposterior (AP)} revealing the classical 'coffee bean' sign (white arrows), diagnostic of sigmoid volvulus; b) 1st look laparoscopic surgical image of the same patient which shows hyper distended sigmoid colon (blue asterisks) in volvulus; c) A 'whirlpooling' (blue arrow) of the root of sigmoid mesocolon in the same patient, also classical of volvulus.

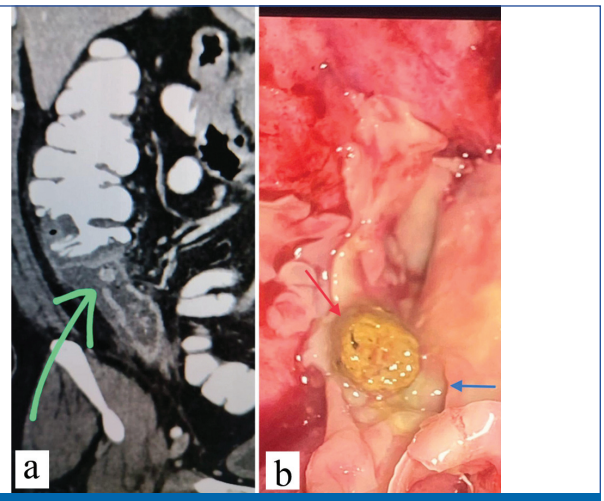

[Table/Fig-8]: Stercoral perforation of appendix: a) CECT scan (coronal view) revealing an obstructing faecolith at the base of the appendix with a breach in its wall near the base (green arrow) indicative of classical stercoral perforation. b) 1st look operative image revealing the faecolith (red arrow) and the perforation (blue arrow).

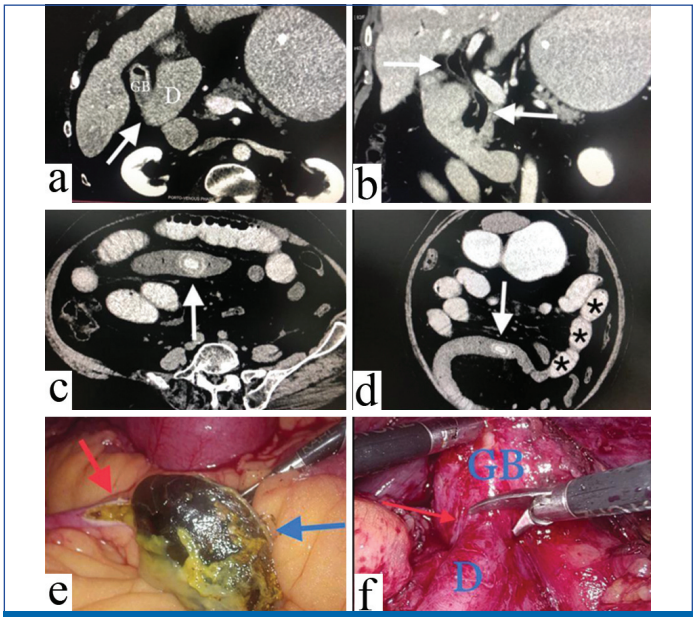

[Table/Fig-9]: Gallstone ileus (Barnard's syndrome): a) CECT scan (axial view) which shows a fistula between the gall bladder and duodenum (white arrow); b) Coronal view is another view of CECT of the same patient showing pneumobilia (white arrows); c) Axial view and d) Coronal view showing lamellated large ectopic stone (white arrow) in the terminal small bowel with dilated proximal ileum (black asterisks). Thus, images b-d complete the classical Rigler's triad of gallstone ileus. e,f) Operative pictures of the same patient; e) Reveals the obstructing large ectopic stone (blue arrow) delivered through an enterotomy (red arrow); f) The cholecystoduodenal fistula being transected (red arrow).

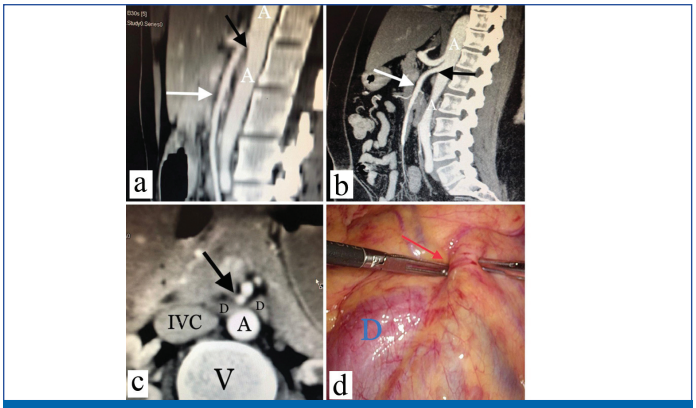

[Table/Fig-10]: Superior mesenteric artery syndrome (Wilkie's syndrome): a) CT mesenteric angiogram (sagittal view) of the patient revealing the aorta, SMA (white arrow) and the markedly reduced aorto-mesenteric angle (black arrow); b) CT mesenteric angiogram (sagittal view) of a normal individual for comparison of the aorto-mesenteric angle (black arrow) with that of the patient a); c) CECT scan axial view showing the compressed 3rd part of duodenum (D3) between the aorta and the SMA (red arrow). d) 1st look surgical image of the same patient revealing the SMA (black arrow) overlying the D3 and dilated proximal duodenum.

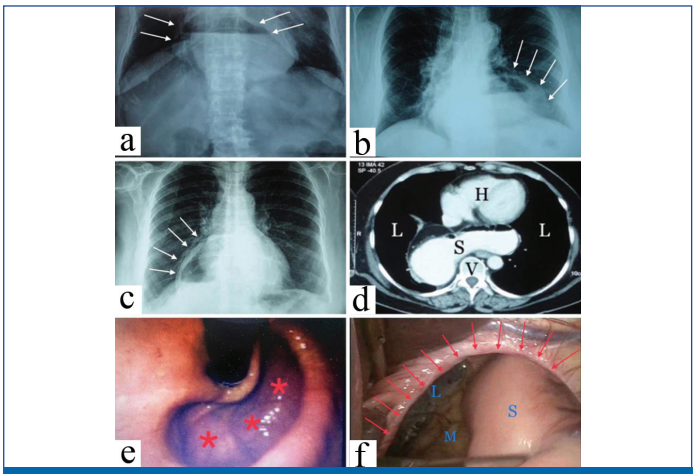

[Table/Fig-11]: Type 2 (Rolling type) hiatus hernia; a-c) Plain X-ray chest {Posteroanterior (PA) view} of 3 different patients revealing the abnormal retrocardiac location of the fundic gas bubble (white arrows), which should ideally lie in the abdomen below the left dome of diaphragm. This is a classical appearance of a type 2 hiatus hernia; d) Axial view of CECT chest of a patient which shows the contrast filled stomach within the chest behind the heart; e) Classical oesophagogastroduodenoscopy image of one of the above 3 patients which shows the fundus and proximal body of stomach rolling and herniating deep into the left chest (red asterisks). f) 1st look laparoscopic surgical image revealing the rolling stomach which has herniated deep through the wide crural/hiatal hernial defect (red arrows). Also, seen are the mediastinum and part of the right lung.

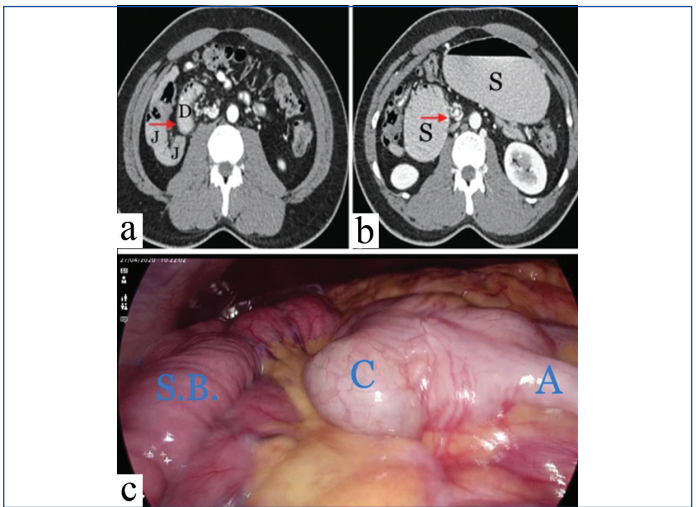

[Table/Fig-12]: Midgut malrotation presenting as acute duodenal obstruction in an adult: a) CECT scan of abdomen (axial view) which reveals the terminal duodenum, duodenojejunal junction (red arrow) and proximal jejunum abnormally continuing down the right side of the patient's abdomen instead of the D3 crossing over back to the left. b) Another axial view of the same patient showing the significantly distended stomach along with the classical whirlpool sign (red arrow); c) Operative 1st look picture which shows Small Bowel (SB) lateral to Caecum (C) and Appendix (A), which is a classic feature of midgut malrotation.

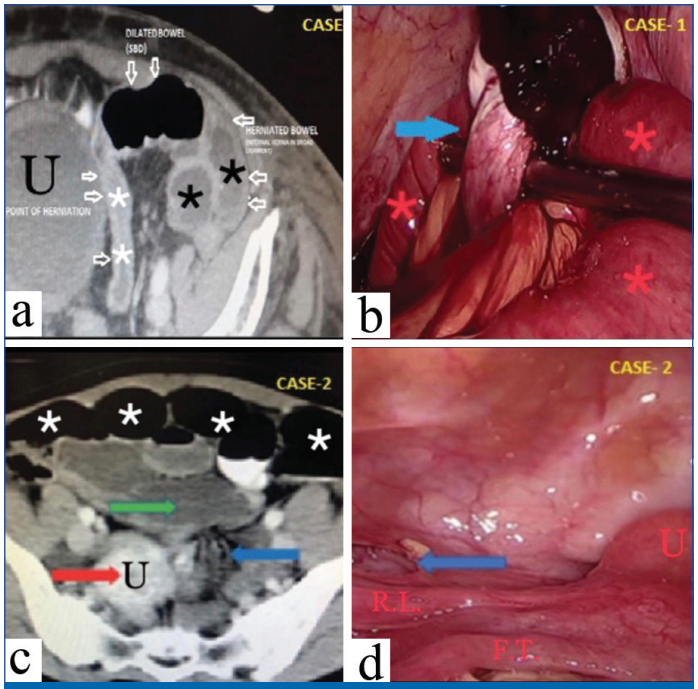

[Table/Fig-13]: Broad Ligament Hernia (BLH): a) Axial view of the CECT pelvis showing the transit point of collapsed (white asterisks) and dilated (black asterisks) small bowel just to the left lateral side of the Uterus (U); b) 1st look operative image of the same patient which shows the entrapped small bowel (red asterisks) within the left-sided BLH defect (blue arrow); c) Axial view of CECT pelvis of another patient with left-sided BLH. It shows whirlpooling of the small bowel mesentery (blue arrow) just to the left lateral side of the Uterus (U). Also, it shows slight right-ward deviation of the uterus (red arrow) classically seen in BLH. It also shows some free fluid in the pelvis (green arrow) along with dilated small bowel loops (white asterisks), typically seen in bowel obstruction. d) Operative 1st look image of the 2nd BLH patient shows the hernia defect (blue arrow). The contents of the hernia spontaneously reduced by the time the authors went in. Also, seen in the vicinity are the Uterus (U), Round Ligament (RL) and the Fallopian Tube (FT).

DISCUSSION

There are certain conditions in which imaging appearances are classical, leading to a quick diagnosis. Legendary are those pathognomonic radiological signs and appearances that have made our lives significantly easier. Herein, the authors salute the torchbearers of the radiological revolution, those whose unparalleled genius and groundbreaking research led to inventions of such monumental significance that they transformed the world of diagnostic imaging and brought about tectonic shifts in related specialties, including surgery. The authors nostalgically and respectfully acknowledge the giants in the field of radiological inventions, as summarised in [Table/Fig-14].

Radiological modality	Inventor/Year of invention/History	Principle	Advantages/ Disadvantages/ Risks/Side-effects
X-rays	German physicist-Wilhelm Conrad Rontgen/1895/won the 1st Nobel prize in Physics in 1901 for it [1]	Use of high energy electromagnetic radiation to produce images of internal tissues on film/digital media	Risks-Dermatitis, hair loss, skin, thyroid cancers, infertility etc.,
Ultrasonography (USG)	1. Engineer Tom Brown and 2. Obstetrician Ian Donald/1956, Glasgow, United Kingdom (UK) 3. John J Wild-father of medical ultrasound, pioneer of USG diagnosis of cancer/early 1950's, Minnesota, United States of America (USA) [2]	Piezoelectric effect-earliest use was as Sound Navigation and Ranging (SONAR) in World war 1 for detecting submarines, also used for ocean floor mapping, advance warning of nearby approaching icebergs etc., [2]	Shortcoming-areas beyond gas filled areas like dilated bowels are blind spots as waves don't penetrate, operator dependant reportage; Advantage-no collateral damage, easily available

Computed Tomography (CT)	1. Engineer Godfrey Hounsfield, UK-CT machine inventor/1971, 2. Physicist Allan Cormack, USA-developed equations pertaining to CT by work on theoretical maths involved in restructuring images using the computer. Both awarded Nobel prize in medicine 1979 [3]	Computerised X-ray imaging procedure- a narrow X-ray beam is aimed at patient and quickly rotated around the body, producing signals that are processed by machine's computer to generate cross sectional images	Risks- same as those of X-rays; Shortcoming- since CT uses X-rays, radiolucent pathology like gallstones are better picked up/ diagnosed on USG Advantages- cutting edge imagery which changed the ball game in radiodiagnostics due to sheer clarity
Magnetic Resonance Imaging (MRI)	1. Raymond Damadian, Physician/inventor of MRI machine/ USA/1974 2. Physicist Isidor Rabi/ USA/discovery of nuclear magnetic resonance/Nobel prize in Physics 1944 3. Chemist Paul Lauterbur/USA/ developed mechanism to encode spatial info into Nuclear Magnetic Resonance (NMR) signal using magnetic field gradients/1971/ Nobel prize for medicine 2003 4. Physicist Peter Mansfield/UK/ inventor of slice selection in MR, understanding of how radio signals frm MR can be mathematically analysed and thereby interpreted into useful image,discovery of fast MR imaging/ Nobel prize for medicine 2003 [4]	Protons of the body get aligned towards magnetic field produced by powerful magnets. When Radiofrequency (RF) current is passed through the patient the protons are stilumated and spin out of equilibrium; straining against the pull of the field. When RF field is turned off, MR sensors are able to detect the energy released as the protons realign with magnetic field. Time taken to realign and energy released changes depending on chemical nature of molecules.	Advantage-Brain, Spinal cord, nerves, muscles, ligaments and tendons more clearly seen with MRI than CT; Shortcoming- cannot be performed for people with non MRI compatible implants like pacemakers, orthopaedic implants, defibrillators, insulin pumps, cochlear implants etc.

[Table/Fig-14]: Role of Radiological honour [1-4].

CONCLUSION(S)

As demonstrated in the present review, a technologically advanced radiological set-up is the backbone of any Surgical Department and hospital. Most of the rare and unique cases presented in the present series would not have been accurately diagnosed preoperatively without the support of the Radiology Department. The timely and precise surgical interventions for all these patients were a logical conclusion to the precision imaging diagnostics provided by the cutting-edge radiological equipment, which is effectively complemented by a dedicated team of radiologists in the present study's Institutional facility.

REFERENCES

[1] Babic RR, Stankovic Babic G, Babic SR, Babic NR. 120 years since the discovery of x-rays. Med Pregl. 2016;69(9-10):323-30.
[2] Newman PG, Rozycki GS. The history of ultrasound. Surg Clin North Am. 1998;78(2):179-95.
[3] Patel PR, De Jesus O. CT Scan. 2023 Jan 2. In: StatPearls [Internet]. Treasure Island (FL): StatPearls Publishing; 2024. PMID: 33620865.
[4] Geva T. Magnetic resonance imaging: Historical perspective. J Cardiovasc Magn Reson. 2006;8(4):573-80.

PARTICULARS OF CONTRIBUTORS:
1. Diplomate in National Board (DNB) General Surgery Resident, Department of General Surgery, Dr. L.H. Hiranandani Hospital, Mumbai, Maharashtra, India.
2. Consultant and Head, Department of Radiology, Dr. L.H. Hiranandani Hospital, Mumbai, Maharashtra, India.
3. Consultant General and Advanced Laparoscopic Surgeon, Department of General Surgery, Dr. L.H. Hiranandani Hospital, Mumbai, Maharashtra, India.

NAME, ADDRESS, E-MAIL ID OF THE CORRESPONDING AUTHOR:
Ravikumar Kalyanbhai Balar,
B601, Cindrella CHS, Powai, Mumbai-400076, Maharashtra, India.
E-mail: ravibalar3895@gmail.com

PLAGIARISM CHECKING METHODS: [Jain H et al.]
- Plagiarism X-checker: Feb 25, 2024
- Manual Googling: Jul 01, 2024
- iThenticate Software: Jul 06, 2024 (1%)

ETYMOLOGY: Author Origin

EMENDATIONS: 6

AUTHOR DECLARATION:
- Financial or Other Competing Interests: None
- Was Ethics Committee Approval obtained for this study? Yes
- Was informed consent obtained from the subjects involved in the study? Yes
- For any images presented appropriate consent has been obtained from the subjects. Yes

Date of Submission: **Feb 25, 2024**
Date of Peer Review: **May 31, 2024**
Date of Acceptance: **Jul 08, 2024**
Date of Publishing: **Sep 01, 2024**